ON-BOARD MULTISPECTRAL ALIGNMENT FOR IMPROVED CLASSIFICATION AND COMPRESSION RESULTS*

Timo Rolf Bretschneider

School of Computer Engineering
Nanyang Technological University
Blk. N4 #02a-32, Nanyang Avenue, Singapore 639798
Tel: +65 – 6790 – 6045 Fax: +65 – 6792 – 6559
E-mail: astimo@ntu.edu.sg
SINGAPORE

KEY WORDS: Multispectral alignment, parallel on-board processing, displacement, small-satellites

ABSTRACT:

In the future the significance of on-board processing of acquired images will increase. The reason is less a changed objective in the user community but rather the rising impact of engineering limitations. Prominent examples are given by micro-, mini-, and small-satellites that are currently gaining in popularity. One of the most substantial implications in the design of these satellites is a limited downlink bandwidth for various reasons, e.g. a restricted power budget and / or a small number of ground receiving stations. Therefore on-board processing becomes almost mandatory since it enables the utilisation of the raw imagery and reduces the amount of data by computing high-level products, which then again eases the requirements on the communication link. The advantages of this approach are predominant for highly specialised missions. However, even for general imaging missions on-board processing can provide additional benefits. This paper illustrates the gains of on-board processing by choosing multispectral alignment as a demonstrating application. The multispectral band-to-band alignment is one key factor in remote sensing and a mismatch between the different spectral bands inevitably leads to decreased accuracy for every application that makes explicitly use of the spectral information. The causes for the displacement are mainly determined by the design of the acquisition unit, i.e. the arrangement of the charge coupled devices. This paper proposes a technique to measure the actual displacement. Subsequently the multispectral scenes are aligned using a parallel processing unit that is currently developed for the mini-satellite mission X-Sat. The results show that satellite missions profit by the on-board alignment since the data reliability is improved. This is of major interest for any further processing of the image data, which will continuously be pushed towards space over the next few years.

1. INTRODUCTION

A constant bottleneck in the design of remote sensing micro-, mini, and small-satellites is the available downlink capacity. Choices are manifold but for many space emerging countries the implicit constraints are difficult to overcome. In general the number of available ground receiving stations for the downlink of the image data is small, i.e. the time the satellite is within the range of the own station is limited. Higher transmission rates ease this problem but have a direct impact on the satellite design since power requirements become difficult to be fulfilled. A similar problem is faced by deep space missions (Manduchi et al. 2000) where the communication limitations are even more severe. One possibility to circumvent the described problem is to tackle the problem directly, i.e. to reduce the amount of data. A conservative approach is image compression, which proofed to be useful in many cases. However, the downlink bottleneck could not be eliminated since information theory determines an upper bound with respect to the achievable compression ration for all lossless compression algorithms. Generally lossy compression is undesirable since it has a direct impact on the subsequently utilised applications. Therefore this paper proposes a different approach. Instead of transferring the acquired data to the ground it is directly processed on board of the satellite. Thus high-level products are created, which generally ease the requirements on the communication link since these products are by magnitudes smaller in volume than the originally raw data. The advantages of this approach are predominant for highly specialised missions – which many of the smaller missions are. The specific focus of the corresponding satellite programmes enables the renunciation of the actual imagery. An example is the

* This work has been partly supported by the German Research Foundation (*Deutsche Forschungsgemeinschaft*).

detection of natural and man-made hazards like bushfires and oil spills. Once a hazard is detected only selected image regions around the particular locations are required.

This paper depicts one key factor for a successful on-board processing strategy – namely the multispectral band-to-band alignment in space. Since most spectral related applications, e.g. ground cover classification and fire detection, require a minimal displacement between corresponding pixels in the different bands, this example is suitable to demonstrate the benefits of the proposed change processing approach: from a purely remote sensing perspective towards a combined *remote sensing and remote processing* tactic.

The causes for the displacement are mainly determined by the design of the actual acquisition unit, i.e. the arrangement of the charge coupled devices (CCD). Two different kinds of discontinuities have to be considered: Firstly the inter-band displacement, which results from the imperfect mounting of the individual scan lines, effects the bands to be globally shifted – and possible slightly rotated – with respect to each other. Secondly the creation of a virtual scan line by using a number of CCDs with the aim to gain a larger swath yields in intra-band discontinuities. Even for professional satellites like SPOT the shift between corresponding pixel centres can mount to $^2/_3$ of a pixel (Bretschneider et al., 2001). The resulting problems from displaced bands are manifold for the subsequently used applications. One example is given by degraded classification accuracy since the pixels exhibit a high degree of mixed spectral classes due to the spatial differences between the observations in each band. Another instance of the problem is that features appear to be more blurred than expected from the Nyquist criterion.

This paper presents a combined software and hardware solution that achieves multispectral alignment on-board of satellites. While the software is tailor-made for the specific problem under consideration, the hardware is a multi-purpose design consisting of several parallel processors, which are supported by field programmable gate arrays (FPGA). The so-called parallel processing unit (PPU) is part of the X-Sat satellite project of Nanyang Technological University and aims to provide sufficient computational resources on-board of small satellites. The launch of the satellite is due for 2006.

The measurement of the displacement is described in Section 2 and employs the computation of the correlation between the distinct spectral bands. For the determination of the correlation peak to sub-pixel accuracy the original imagery is oversampled. The calculation uses sub-images from the real imagery because the displacement is space-variant. To obtain a sharper correlation peak and to exclude the influence of the different spectral histograms, gradient images are used. An additional minimisation between the actual correlation peak and the expected characteristic increases the accuracy furthermore. After the estimation of the displacement the individual bands are resampled to align corresponding pixels. The hardware layout and the mapping of the algorithm on the particular architecture are illustrated in Section 3 with the particular emphasis on realtime processing, i.e. simultaneous imaging and alignment. One main consideration is the parallelisation of the algorithm. Subsequently Section 4 investigates the impact of the alignment on the data. Finally conclusions are given in Section 5.

2. MULTISPECTRAL DISPLACEMENT

The usability of multispectral imagery for application which exploit the spectral information content highly depend on the spatial offset between the spectral bands. As mentioned by Billingsley (Billingsley, 1982) alignment between the bands has to be better than 0.1-0.2 pixel for precise classification. However, even the well-known SPOT satellite only guarantees that the centres of three corresponding pixels in the different bands fall within a circle with a radius up to a third of a pixel (SPOT Image, 1988). Thus in the worst case two pixel centres might be displaced by $^2/_3$ of the pixel spacing which is equivalent to approximately 13m on the ground. An in-depth analysis for SPOT is provided in (Bretschneider et al., 2001).

2.1. Measurement of the Displacement

The measurement of the displacement employs the computation of the correlation between the distinct spectral bands. The calculation uses sub-images f from the real imagery because the displacement is space-variant and depends especially on the CCD arrays. For the determination of the correlation peak to sub-pixel accuracy the imagery is oversampled by a factor of 16. A Kaiser-weighted sinc function is employed for the interpolation since the resulting kernel approximates the sinc-function with its infinite extent more accurately than for example cubic or B-spline interpolators. Equation (1) shows the one-dimensional Kaiser window W with extent k and the definition of the sinc function. I_0 is the zeroth order

Bessel function of the first kind and a the window parameter. The product of both functions gives the actual interpolation kernel and is easily extended to the required two-dimensional version.

$$W(x) = \begin{cases} I_0\left(\alpha\sqrt{1-(x/k)^2}\right)/I_0(\alpha) & |x| \le k \\ 0 & |x| > k \end{cases} \qquad (1)$$
$$\operatorname{sinc}(x) = \sin(\pi x)/\pi x \qquad \operatorname{sinc}(1) = 1$$

Therefore the oversampled image f_S is described by

$$f_S(x,y) = f_N(x,y) \otimes (W(x,y) \cdot \operatorname{sinc}(x)), \qquad (2)$$

where f_N is a special version of the input image f filled with zeros at the interpolation positions. To reduce the influence of the different spectral content between the individual bands, gradient images are used before the actual correlation image is computed, i.e.

$$f_G(x,y) = \sqrt{\left(\frac{\partial f_S(x,y)}{\partial x}\right)^2 + \left(\frac{\partial f_S(x,y)}{\partial y}\right)^2}. \qquad (3)$$

The underlying assumption is that spatial features are depicted throughout all bands whereby this similarity has to extend to high spatial frequencies. Note that the symmetric gradient is used to avoid shifts. Equation (4) depicts the gradient for the x-direction with M being the number of pixel columns in an arbitrary image f. The definition for the y-direction is equivalent.

$$\frac{\partial f(x,y)}{\partial x} = \begin{cases} f(x+1,y) - f(x,y) & x = 1 \\ (f(x+1,y) - f(x-1,y))/2 & 1 < x < M \\ f(x,y) - f(x-1,y) & x = M \end{cases}. \qquad (4)$$

Finally the correlation image c is computed using

$$c(x,y) = f_G(x,y) \star g_G(x,y), \qquad (5)$$

where f_G and g_G are corresponding gradient images from the oversampled sub-scenes, which were originally extracted from different bands. Finally a quadratic surface, which is described by the coefficients a_i, is fitted to the centre of the correlation peak p using

$$\min_{a_i} \mathrm{E}\left(a_0 + a_1 x^2 + a_2 y^2 + a_3 x + a_4 y + a_5 xy - p(x,y)\right)^2, \qquad (6)$$

whereby the minimisation over the a_i is performed using the Nelder-Mead-Simples algorithm (Nelder and Mead, 1965). The actual displacement is determined by the spatial offset between the maximum location of the quadratic surface and the theoretical centre of the correlation image. Simulations proved that the fitting of the quadratic surface together with the interpolation leads to an accuracy of approximately $^1/_{50}^{\text{th}}$ of a pixel.

The actual implementation of Equation (1) – (5) uses the convolution and correlation theorem, i.e.

$$\begin{aligned} c(x,y) &= f(x,y) \otimes g(x,y) \leftrightarrow C(u,v) = F(u,v) \cdot G(u,v), \\ c(x,y) &= f(x,y) \star g(x,y) \leftrightarrow C(u,v) = F^*(u,v) \cdot G(u,v), \end{aligned} \qquad (7)$$

where G and F are the Fourier transforms of the corresponding lower case variables. The symbol $\leftrightarrow$ represents the Fourier and inverse Fourier transformation, respectively. The advantage is a fast computation since only point-wise multiplication is required. The incorporation of the interpolation and gradient calculation is straightforward.

2.2. Sub-Pixel Alignment

In the previous sub-section the computation of the displacement for arbitrary sub-scenes was described. However, the alignment of the bands to sub-pixel accuracy requires a well-defined function that describes the actual displacement. The derivation of this function is explained subsequently. The vast majority of nowadays scanning system is using the push-broom principle, which acquires a whole

image line in the across-track direction at one moment of time. Therefore the inter-band displacement has to be the same for every single image line. However, in practice the measurements of the displacement for the sub-images, which are aligned in the along-track direction, vary because high intensity values within the images bias the location of the correlation peak. To overcome this problem the computation is performed for several sub-images with distinct along-track coordinates and finally the mean values $\bar{x}$ and $\bar{y}$ are assumed to be a representative measurement.

An analysis of the gained displacement data for the push-broom scanners SPOT and MOMS revealed that the calculation only has to be repeated for a carefully chosen set of location, i.e. sub-images should not overlap with the inherent image boundaries if several CCDs are used to form a virtual scan line. Assuming a linear model to specify the actual displacement a line with its describing parameters m and b can be fitted through the measured data, i.e.

$$\begin{pmatrix} \bar{x}_1 \\ \vdots \\ \bar{x}_N \end{pmatrix} = \begin{bmatrix} x_1 & 1 \\ \vdots & \vdots \\ x_N & 1 \end{bmatrix} \begin{pmatrix} m_x \\ b_x \end{pmatrix} \quad \text{and} \quad \begin{pmatrix} \bar{y}_1 \\ \vdots \\ \bar{y}_N \end{pmatrix} = \begin{bmatrix} y_1 & 1 \\ \vdots & \vdots \\ y_N & 1 \end{bmatrix} \begin{pmatrix} m_y \\ b_y \end{pmatrix}, \tag{8}$$

whereby the x_i and y_i are the N positions within the image for which the displacements in the across-track direction x and the along-track direction y were measured. Since N should be significantly larger than the order of the model, the pseudo-inverse has to be utilised to solve for the parameters m and b. Note that the displacement generally does not vary significantly over short periods of time as long as no major changes in the environmental conditions occurred. Therefore the displacement can be assumed to be known after regular assessments of the actual shift among corresponding pixels.

The alignment of the multispectral bands uses the gained information about the actual displacement in terms of the two variable pairs (m_x,b_x) and (m_y,b_y). All bands are resampled with respect to the pixel centres of the first band, whereby the described Kaiser-weighed sinc interpolator in Equation (1) is utilised.

3. ON-BOARD HARDWARE ARCHITECTURE

The parallel processing unit* (PPU) consists of four fully connected radiation-hardened FPGA with each of it hosting four processing nodes (PN). Every $PN_{i,j}$ comprises a StrongArm processor and 64 MByte of local memory. The resulting architecture is a 4×4 mesh with wrap-around since the intra-FPGA connections have four times the bandwidth of the PN-FPGA interconnections. In addition every $FGPA_i$ accommodates a spare processor node SN_i in case a regular PN becomes inoperative due to radiation. The system is designed as payload and is connected to a bulk storage module called RAM-Disk by two interfaces, which allow simultaneous read-write-operations. Therefore the PPU is perfectly suited to perform realtime tasks by directly processing the incoming dataflow from the camera. The connection to the controlling on-board computer (OBC) is realised by a CAN interface with a secondary interface as backup system. Figure 1 shows an overview of the system architecture.

* Credits for the design of the PPU are to Ian McLoughlin and the Satellite Engineering Centre of Nanyang Technological University, Singapore

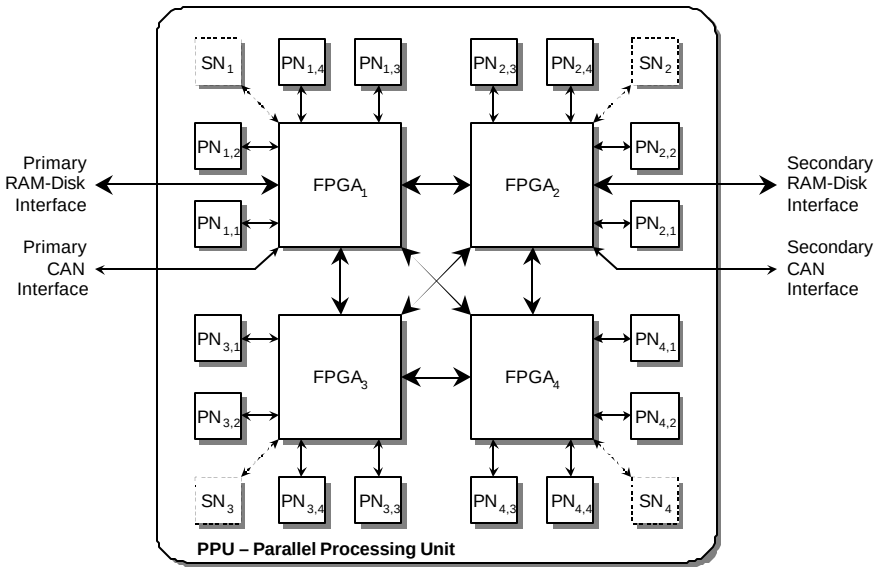

Figure 1: Schematic of the future parallel processing unit on board of X-Sat

For simplicity each PN runs its own instance of the realtime operating system VxWorks. The system provides according to Flynn's taxonomy MIMD (multiple instructions multiple data) capability but also caters for SIMD (single instructions multiple data) and pipelined processing. Currently not all components of the system are available and therefore a simulated model of the PPU was created using OMNET++[**].

The multispectral camera has three bands with a spectral characteristic that is similar to the SPOT design. The bands are acquired by individual CCD lines, which are mounted on a prism. Like reported for the SPOT camera (Bretschneider et al., 2001) this design approach leads to considerable misalignments and therefore requires a resampling of the bands before the data can be utilised. The imaging instrument provides a constant stream of data, however, the on-board storage capacities are limited and only allow a storage equivalent of ten minutes of consecutive acquisition. Therefore the data has to be processed in realtime to enable the mission goals, e.g. detection of features according to their spectral signatures and three-dimensional image compression. This paper focuses solely on the on-board multispectral alignment. For further applications of the PPU refer to (Bretschneider, 2002) and (Trenschel et al., 2002).

The simulations found that a simple round-robin streaming of image stripes to individual processors provides the best performance. Each strip covers the entire swath, which results in an optimal RAM disk access. While the data is read using the primary RAM-Disk interface, the aligned data and/or the results are stored using the secondary interface to the bulk storage module. The number of lines per strip highly depends on the available number of PNs, the actual algorithm, which utilises the corrected data, as well as the tolerated latency of the processing. Figure 2 provides a schematic of the data flow. Note that every PN is acquainted with the displacement values, which – like mentioned previously – are assumed to be constant over a certain time interval.

[**] http://www.hit.bme.hu/phd/vargaa/omnetpp/

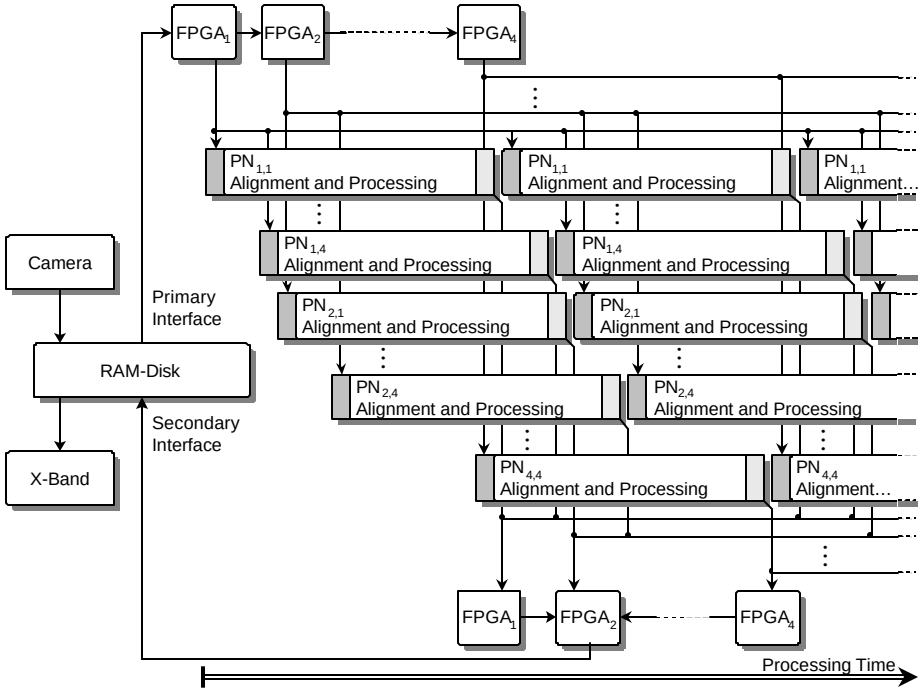

Figure 2: Streaming of the image data to the PNs

A constant streaming of the data through the PPU is enabled due to the separate connections of the primary and secondary RAM-Disk interface to individual FPGAs. However, one image data assignment cycle is required before the entire computational resources are utilised. Note that the FPGAs are not only responsible for the routing but also enable the implementation of an efficient pre-processing stage, e.g. radiometric calibration, before the data reaches the actual PN. This additional functionality comes without any further costs in terms of data throughput and can decrease the overall computation time significantly.

4. CLASSIFICATION AND COMPRESSION IMPROVEMENTS

All algorithms that exploit the spectral characteristic of the data rely on the spatial alignment of corresponding pixels. This holds true in particular for techniques, which are based on the sub-pixel scale, e.g. sub-pixel detection (Chang and Heinz, 2000) and sub-pixel classification (Tatem et al., 2001).

Generally the absolute value of the correlation increases if the size of the corresponding area is decreased, i.e. locally there is a high similarity even between bands of different wavelength ranges. A simple example is depicted by edges in the imagery, which are observable in most of the bands. A displacement between the bands leads to irrelevant values since – with respect to the edges – the features are blurred. In Figure 3 the standard deviation σ of the local correlations $c_{n\times n}$ versus the length n of the local $n\times n$ window is shown. The larger values for small window sizes are an indication for desired data vivacity since purely correlated bands – and thus a low σ – are not of major use for classification purposes. However, part of this entropy is based on the band displacement. After the alignment of corresponding pixels these distortions are removed without altering the actual statistic of the underlying data, i.e. the two curves in Figure 3 exhibit a similar overall characteristic.

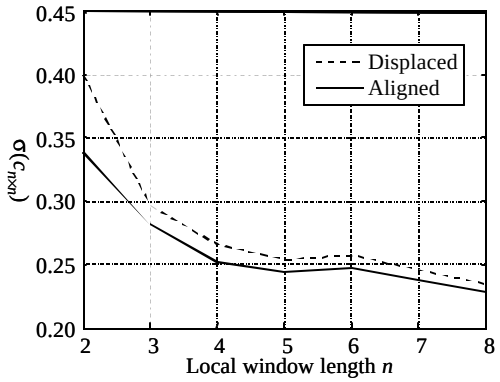

Figure 3: Standard deviation of the local correlation

5. CONCLUSIONS

A technique to estimate sub-pixel displacement between simultaneously acquired multispectral bands was presented. The gained information was used to resample the bands to a common coordinate system and thus to align corresponding pixel. This pre-processing is mandatory for all applications, which rely on pure spectral signatures, whereby mixed-pixels only occur due to the lack in spatial resolution.

The main contribution of the paper is the transfer of the data processing on the ground to an on-board solution. The required hardware with the matching mapping of the software on the actual hardware was described. The foremost reason for on-board processing is the increasing significance of design constraints in mini-satellites, e.g. more data can be acquired than downlinked. Nevertheless relaxation of the problem can be achieved if only high-level products with a reduced data volume are transmitted to the ground station. The proposed system is a first step towards this goal and demonstrates the principal feasibility of remote processing.

REFERENCES

Billingsley, F.C., 1982. Modeling misregistration and related effects on multispectral classification. Photo-grammetry Engineering and Remote Sensing, 48, pp. 421–430.

Bretschneider, T., Bones, P.J., McNeill, S., Pairman, D., 2001. Image-based quality assessment of SPOT data. Proceedings of the American Society for Photogrammetry and Remote Sensing, Sensor and Image Quality Considerations, CD-ROM.

Bretschneider, T., 2002. Blur identification in satellite imagery using image doublets. To be published in the Proceedings of the Asian Conference on Remote Sensing, Kathmandu, Nepal.

Chang C.-I., Heinz, D., 2000. Subpixel spectral detection for remotely sensed images. IEEE Transactions on Geoscience and Remote Sensing, 38(3), pp. 1144– 1159.

Manduchi, R., Dolinar, S., Pollara, F., Matache, A., 2000. Onboard science processing and buffer management for intelligent deep space communications. Proceedings of the IEEE Aerospace Conference, 1, pp. 329–339.

SPOT Image, 1988. SPOT user's handbook. Centre National d'Etude Spatiale (CNES) and SPOT Image, France.

Tatem, A.J., Lewis, H.G., Atkinson, P.M., Nixon, M.S., 2001. Super-resolution mapping of multiple-scale land cover features using a Hopfield neural network. IEEE Proceedings of the International Geoscience and Remote Sensing Symposium, 7, pp. 3200–3202.

Trenschel, T., Bretschneider, T., Leedham, G., 2002. Application specific compression for mini-satellites with limited downlink capacity. To be published in the Proceedings of the Asian Conference on Remote Sensing, Kathmandu, Nepal.